

[Stable continuous-wave single-frequency intracavity frequency-doubled laser with intensity noise suppressed in audio frequency region](#)

Ying-Hao Gao(高英豪), Yuan-Ji Li(李渊骥), Jin-Xia Feng(冯晋霞), Kuan-Shou Zhang(张宽收)

Citation: Chin. Phys. B . 2019, 28(9): 094204 . doi: 10.1088/1674-1056/28/9/094204

Journal homepage: <http://cpb.iphy.ac.cn>; <http://iopscience.iop.org/cpb>

What follows is a list of articles you may be interested in

[Multi-wavelength continuous-wave Nd:YVO₄ self-Raman laser under in-band pumping](#)

Li Fan(樊莉), Xiao-Dong Zhao(赵孝冬), Yun-Chuan Zhang(张蕴川), Xiao-Dong Gu(顾晓东), Hao-Peng Wan(万浩鹏), Hui-Bo Fan(范会博), Jun Zhu(朱骏)

Chin. Phys. B . 2019, 28(8): 084210 . doi: 10.1088/1674-1056/28/8/084210

[High power diode-pumped passively mode-locked Nd:YVO₄ laser at repetition rate of 3.2 GHz](#)

Meng-Yao Cheng(程梦尧), Zhao-Hua Wang(王兆华), Yan-Fang Cao(曹艳芳), Xiang-Hao Meng(孟祥昊), Jiang-Feng Zhu(朱江峰), Jun-Li Wang(王军利), Zhi-Yi Wei(魏志义)

Chin. Phys. B . 2019, 28(5): 054205 . doi: 10.1088/1674-1056/28/5/054205

[Linear polarization output performance of Nd: YAG laser at 946 nm considering the energy-transfer upconversion](#)

Jin-Xia Feng(冯晋霞), Yuan-Ji Li(李渊骥), Kuan-Shou Zhang(张宽收)

Chin. Phys. B . 2018, 27(7): 074211 . doi: 10.1088/1674-1056/27/7/074211

[High-power ultraviolet 278-nm laser from fourth-harmonic generation of an Nd: YAG amplifier in CsB₃O₅ crystal](#)

Miao He(何苗), Feng Yang(杨峰), Cheng Dong(董程), Zhi-Chao Wang(王志超), Lei Yuan(袁磊), Yi-Ting Xu(徐一汀), Guo-Chun Zhang(张国春), Zhi-Min Wang(王志敏), Yong Bo(薄勇), Qin-Jun Peng(彭钦军), Da-Fu Cui(崔大复), Yi-Cheng Wu(吴以成), Zu-Yan Xu(许祖彦)

Chin. Phys. B . 2018, 27(5): 054211 . doi: 10.1088/1674-1056/27/5/054211

[Er³⁺, Yb³⁺:glass-Co²⁺:MgAl₂O₄ diffusion bonded passively Q-switched laser](#)

Yan Zou(邹岩), Yong-Ling Hui(惠勇凌), Jin-Lu Cai(蔡瑾鹭), Na Guo(郭娜), Meng-Hua Jiang(姜梦华), Hong Lei(雷雷), Qiang Li(李强)

Chin. Phys. B . 2017, 26(9): 094206 . doi: 10.1088/1674-1056/26/9/094206

CPB

Chinese Physics B

Volume 28 September 2019 Number 9

TOPICAL REVIEW

- A celebration of the 100th birthday of Kun Huang

SPECIAL TOPIC

- Strong-field atomic and molecular physics
- 110th Anniversary of Lanzhou University

A series Journal of the Chinese Physical Society Distributed by IOP Publishing

iopscience.org/cpb | cpb.iphy.ac.cn

Featured Article

Manipulation of superconducting qubit with direct digital synthesis

Zhi-Yuan Li, Hai-Feng Yu, Xin-Sheng Tan, Shi-Ping Zhao and Yang Yu

Chin. Phys. B, 2019, 28 (9): 098505

Chinese Physics B (中国物理 B)

Published monthly in hard copy by the Chinese Physical Society and online by IOP Publishing, Temple Circus, Temple Way, Bristol BS1 6HG, UK

Institutional subscription information: 2019 volume

For all countries, except the United States, Canada and Central and South America, the subscription rate per annual volume is UK£974 (electronic only) or UK£1063 (print + electronic).

Delivery is by air-speeded mail from the United Kingdom.

Orders to:

Journals Subscription Fulfilment, IOP Publishing, Temple Circus, Temple Way, Bristol BS1 6HG, UK

For the United States, Canada and Central and South America, the subscription rate per annual volume is US\$1925 (electronic only) or US\$2100 (print + electronic). Delivery is by transatlantic airfreight and onward mailing.

Orders to: IOP Publishing, P. O. Box 320, Congers, NY 10920-0320, USA

© 2019 Chinese Physical Society and IOP Publishing Ltd

All rights reserved. No part of this publication may be reproduced, stored in a retrieval system, or transmitted in any form or by any means, electronic, mechanical, photocopying, recording or otherwise, without the prior written permission of the copyright owner.

Supported by the China Association for Science and Technology and Chinese Academy of Sciences

Editorial Office: Institute of Physics, Chinese Academy of Sciences, P. O. Box 603, Beijing 100190, China

Tel: (86-10) 82649026 or 82649519, Fax: (86-10) 82649027, E-mail: cpb@aphy.iphy.ac.cn

主管单位: 中国科学院

国际统一刊号: ISSN 1674-1056

主办单位: 中国物理学会和中国科学院物理研究所

国内统一刊号: CN 11-5639/O4

主 编: 欧阳钟灿

编辑部地址: 北京 中关村 中国科学院物理研究所内

出 版: 中国物理学会

通 讯 地 址: 100190 北京 603 信箱

印刷装订: 北京科信印刷有限公司

电 话: (010) 82649026, 82649519

编 辑: Chinese Physics B 编辑部

传 真: (010) 82649027

国内发行: Chinese Physics B 出版发行部

“Chinese Physics B”网址:

国外发行: IOP Publishing Ltd

<http://cpb.iphy.ac.cn>

发行范围: 公开发售

<http://iopscience.iop.org/journal/1674-1056>

Published by the Chinese Physical Society

Advisory Board

Prof. Academician Chen Jia-Er(陈佳洱)

School of Physics, Peking University, Beijing 100871, China

Prof. Academician Feng Duan(冯端)

Department of Physics, Nanjing University, Nanjing 210093, China

Prof. Academician T. D. Lee(李政道)

Department of Physics, Columbia University, New York, NY 10027, USA

Prof. Academician Samuel C. C. Ting(丁肇中)

LEP3, CERN, CH-1211, Geneva 23, Switzerland

Prof. Academician C. N. Yang(杨振宁)

Institute for Theoretical Physics, State University of New York, USA

Prof. Academician Yang Fu-Jia(杨福家)

Department of Nuclear Physics, Fudan University, Shanghai 200433, China

Prof. Academician Zhou Guang-Zhao

China Association for Science and Technology, Beijing 100863, China

(Chou Kuang-Chao)(周光召)

Prof. Academician Wang Nai-Yan(王乃彦)

China Institute of Atomic Energy, Beijing 102413, China

Prof. Academician Liang Jing-Kui(梁敬魁)

Institute of Physics, Chinese Academy of Sciences, Beijing 100190, China

Editor-in-Chief

Prof. Academician Ouyang Zhong-Can(欧阳钟灿)

Institute of Theoretical Physics, Chinese Academy of Sciences, Beijing 100190, China

Associate Editors

- Prof. Academician Zhao Zhong-Xian(赵忠贤) Institute of Physics, Chinese Academy of Sciences, Beijing 100190, China
Prof. Academician Yang Guo-Zhen(杨国桢) Institute of Physics, Chinese Academy of Sciences, Beijing 100190, China
Prof. Academician Zhang Jie(张杰) Chinese Academy of Sciences, Beijing 100864, China
Prof. Academician Xing Ding-Yu(邢定钰) Department of Physics, Nanjing University, Nanjing 210093, China
Prof. Academician Shen Bao-Gen(沈保根) Institute of Physics, Chinese Academy of Sciences, Beijing 100190, China
Prof. Academician Gong Qi-Huang(龚旗煌) School of Physics, Peking University, Beijing 100871, China
Prof. Academician Xue Qi-Kun(薛其坤) Department of Physics, Tsinghua University, Beijing 100084, China
Prof. Sheng Ping(沈平) The Hong Kong University of Science & Technology, Kowloon, Hong Kong, China

Editorial Board

- Prof. David Andelman School of Physics and Astronomy Tel Aviv University, Tel Aviv 69978, Israel
Prof. Academician Chen Xian-Hui(陈仙辉) Department of Physics, University of Science and Technology of China, Hefei 230026, China
Prof. Cheng Jian-Chun(程建春) School of Physics, Nanjing University, Nanjing 210093, China
Prof. Chia-Ling Chien Department of Physics and Astronomy, The Johns Hopkins University, Baltimore, MD 21218, USA
Prof. Dai Xi(戴希) Institute of Physics, Chinese Academy of Sciences, Beijing 100190, China
Prof. Ding Jun(丁军) Department of Materials Science & Engineering, National University of Singapore, Singapore 117576, Singapore
Prof. Masao Doi Toyota Physical and Chemical Research Institute, Yokomichi, Nagakute, Aichi 480-1192, Japan
Prof. Fang Zhong(方忠) Institute of Physics, Chinese Academy of Sciences, Beijing 100190, China
Prof. Feng Shi-Ping(冯世平) Department of Physics, Beijing Normal University, Beijing 100875, China
Prof. Academician Gao Hong-Jun(高鸿钧) Institute of Physics, Chinese Academy of Sciences, Beijing 100190, China
Prof. Gu Chang-Zhi(顾长志) Institute of Physics, Chinese Academy of Sciences, Beijing 100190, China
Prof. Gu Min(顾敏) Royal Melbourne Institute of Technology (RMIT University), GPO Box 2476, Melbourne, VIC 3001, Australia
Prof. Academician Guo Guang-Can(郭光灿) School of Physical Sciences, University of Science and Technology of China, Hefei 230026, China
Prof. Academician He Xian-Tu(贺贤土) Institute of Applied Physics and Computational Mathematics, Beijing 100088, China
Prof. Werner A. Hofer Stephenson Institute for Renewable Energy, The University of Liverpool, Liverpool L69 3BX, UK
Prof. Hong Ming-Hui(洪明辉) Department of Electrical and Computer Engineering, National University of Singapore, Singapore 117576, Singapore
Prof. Hu Gang(胡岗) Department of Physics, Beijing Normal University, Beijing 100875, China
Prof. Jiang Hong-Wen(姜弘文) Department of Physics and Astronomy, University of California, Los Angeles, CA 90095, USA
Prof. Jiang Ying(江颖) School of Physics, Peking University, Beijing 100871, China
Prof. Jin Xiao-Feng(金晓峰) Department of Physics, Fudan University, Shanghai 200433, China
Prof. Robert J. Joynt Physics Department, University of Wisconsin-Madison, Madison, USA
Prof. Jaewan Kim Korea Institute for Advanced Study, School of Computational Sciences, Hoegiro 85, Seoul 02455, Korea
Prof. Li Ru-Xin(李儒新) Shanghai Institute of Optics and Fine Mechanics, Chinese Academy of Sciences, Shanghai 201800, China
Prof. Li Xiao-Guang(李晓光) Department of Physics, University of Science and Technology of China, Hefei 230026, China
Assits. Prof. Liu Chao-Xing(刘朝星) Department of Physics, Pennsylvania State University, PA 16802-6300, USA
Prof. Liu Xiang-Yang(刘向阳) Department of Physics, Xiamen University, Xiamen 361005, China
Prof. Liu Ying(刘荧) Department of Physics and Astronomy, Shanghai Jiao Tong University, Shanghai 200240, China
Prof. Long Gui-Lu(龙桂鲁) Department of Physics, Tsinghua University, Beijing 100084, China
Prof. Lv Li(吕力) Institute of Physics, Chinese Academy of Sciences, Beijing 100190, China
Prof. Ma Xu-Cun(马旭村) Department of Physics, Tsinghua University, Beijing 100084, China
Prof. Antonio H. Castro Neto Physics Department, Faculty of Science, National University of Singapore, Singapore 117546, Singapore
Prof. Nie Yu-Xin(聂玉昕) Institute of Physics, Chinese Academy of Sciences, Beijing 100190, China
Prof. Niu Qian(牛谦) Department of Physics, University of Texas, Austin, TX 78712, USA
Prof. Academician Ouyang Qi(欧阳颀) School of Physics, Peking University, Beijing 100871, China

- Prof. Academician Pan Jian-Wei(潘建伟) Department of Modern Physics, University of Science and Technology of China, Hefei 230026, China
- Prof. Amalia Patane School of Physics and Astronomy, The University of Nottingham, NG7 2RD, UK
- Prof. Qian Lie-Jia(钱列加) Department of Physics and Astronomy, Shanghai Jiao Tong University, Shanghai 200240, China
- Prof. J. Y. Rhee Department of Physics, Sungkyunkwan University, Suwon, Korea
- Prof. Shen Jian(沈健) Department of Physics, Fudan University, Shanghai 200433, China
- Prof. Shen Yuan-Rang(沈元壤) Lawrence Berkeley National Laboratory, Berkeley, CA 94720, USA
- Prof. Shen Zhi-Xun(沈志勋) Stanford University, Stanford, CA 94305-4045, USA
- Prof. Academician Sun Chang-Pu(孙昌璞) Beijing Computational Science Research Center, China Academy of Engineering Physics, Beijing 100094, China
- Prof. Sun Xiao-Wei(孙小卫) Department of Electrical and Electronic Engineering, Southern University of Science and Technology, Shenzhen 518055, China
- Prof. Sun Xiu-Dong(孙秀冬) Department of Physics, Harbin Institute of Technology, Harbin 150001, China
- Prof. Michiyoshi Tanaka Research Institute for Scientific Measurements, Tohoku University, Katahira 2-1-1, Aoba-ku 980, Sendai, Japan
- Prof. Tong Li-Min(童利民) Department of Optical Engineering, Zhejiang University, Hangzhou 310027, China
- Prof. Tong Peng'er(童彭尔) Department of Physics, The Hong Kong University of Science and Technology, Kowloon, Hong Kong, China
- Prof. Wang Bo-Gen(王伯根) School of Physics, Nanjing University, Nanjing 210093, China
- Prof. Wang Kai-You(王开友) Institute of Semiconductors, Chinese Academy of Sciences, Beijing 100083, China
- Prof. Wang Wei(王炜) School of Physics, Nanjing University, Nanjing 210093, China
- Prof. Wang Ya-Yu(王亚愚) Department of Physics, Tsinghua University, Beijing 100084, China
- Prof. Wang Yu-Peng(王玉鹏) Institute of Physics, Chinese Academy of Sciences, Beijing 100190, China
- Prof. Wang Zhao-Zhong(王肇中) Laboratory for Photonics and Nanostructures (LPN) CNRS-UPR20, Route de Nozay, 91460 Marcoussis, France
- Prof. Academician Wang Wei-Hua(汪卫华) Institute of Physics, Chinese Academy of Sciences, Beijing 100190, China
- Prof. Wei Su-Huai(魏苏淮) Beijing Computational Science Research Center, China Academy of Engineering Physics, Beijing 100094, China
- Prof. Wen Hai-Hu(闻海虎) Department of Physics, Nanjing University, Nanjing 210093, China
- Prof. Wu Nan-Jian(吴南健) Institute of Semiconductors, Chinese Academy of Sciences, Beijing 100083, China
- Prof. Academician Xia Jian-Bai(夏建白) Institute of Semiconductors, Chinese Academy of Sciences, Beijing 100083, China
- Prof. Academician Xiang Tao(向涛) Institute of Physics, Chinese Academy of Sciences, Beijing 100190, China
- Prof. Academician Xie Si-Shen(解思深) Institute of Physics, Chinese Academy of Sciences, Beijing 100190, China
- Prof. Academician Xie Xin-Cheng(谢心澄) Department of Physics, Peking University, Beijing 100871, China
- Prof. Academician Xu Zhi-Zhan(徐至展) Shanghai Institute of Optics and Fine Mechanics, Chinese Academy of Sciences, Shanghai 201800, China
- Assist. Prof. Xu Cen-Ke(许岑珂) Department of Physics, University of California, Santa Barbara, CA 93106, USA
- Prof. Academician Ye Chao-Hui(叶朝辉) Wuhan Institute of Physics and Mathematics, Chinese Academy of Sciences, Wuhan 430071, China
- Prof. Ye Jun(叶军) Department of Physics, University of Colorado, Boulder, Colorado 80309-0440, USA
- Prof. Yu Ming-Yang(郁明阳) Theoretical Physics I, Ruhr University, D-44780 Bochum, Germany
- Prof. Academician Zhan Wen-Long(詹文龙) Chinese Academy of Sciences, Beijing 100864, China
- Prof. Zhang Fu-Chun(张富春) Kavli Institute for Theoretical Sciences, University of Chinese Academy of Sciences, Beijing 100190, China
- Prof. Zhang Xiang(张翔) NSF Nanoscale Science and Engineering Center (NSEC), University of California, Berkeley, CA 94720, USA
- Prof. Zhang Yong(张勇) Electrical and Computer Engineering Department, The University of North Carolina at Charlotte, Charlotte, USA
- Prof. Zhang Zhen-Yu(张振宇) International Center for Quantum Design of Functional Materials, University of Science and Technology of China, Hefei 230026, China
- Prof. Zeng Hao(曾浩) Department of Physics, University at Buffalo, SUNY, Buffalo, NY 14260, USA
- Prof. Zheng Bo(郑波) Physics Department, Zhejiang University, Hangzhou 310027, China
- Prof. Zhou Xing-Jiang(周兴江) Institute of Physics, Chinese Academy of Sciences, Beijing 100190, China
- Prof. Academician Zhu Bang-Fen(朱邦芬) Department of Physics, Tsinghua University, Beijing 100084, China

Editorial Staff

Wang Jiu-Li(王久丽) (Editorial Director) Cai Jian-Wei(蔡建伟) Zhai Zhen(翟振)

Stable continuous-wave single-frequency intracavity frequency-doubled laser with intensity noise suppressed in audio frequency region*

Ying-Hao Gao(高英豪)¹, Yuan-Ji Li(李渊骥)^{1,2,†}, Jin-Xia Feng(冯晋霞)^{1,2}, and Kuan-Shou Zhang(张宽收)^{1,2}

¹State Key Laboratory of Quantum Optics and Quantum Optics Devices, Institute of Opto-Electronics, Shanxi University, Taiyuan 030006, China

²Collaborative Innovation Center of Extreme Optics, Shanxi University, Taiyuan 030006, China

(Received 15 March 2019; revised manuscript received 26 June 2019; published online 7 August 2019)

We demonstrated a continuous wave (cw) single-frequency intracavity frequency-doubled Nd:YVO₄/LBO laser with 532 nm output of 7.5 W and 1.06 μm output of 3.1 W, and low intensity noise in audio frequency region. To suppress the intensity noise of the high power 532 nm laser, a laser frequency locking system and a feedback loop based on a Mach-Zehnder interferometer were designed and used. The influences of the frequency stabilization and the crucial parameters of the MZI, such as the power splitting ratio of the beam splitters and the locking state of the MZI, on the intensity noise of the 532 nm laser were investigated in detail. After the experimental optimizations, the laser intensity noise in the frequency region from 0.4 kHz to 10 kHz was significantly suppressed.

Keywords: continuous wave single-frequency intracavity frequency-doubled laser, noise suppression, power stabilization, audio frequency

PACS: 42.55.Xi, 42.65.Ky, 42.50.Lc

DOI: 10.1088/1674-1056/ab327b

1. Introduction

Continuous-wave (cw) single-frequency all-solid-state lasers with the features of low noise, good beam quality, and long coherent length have found applications in a number of fields, including quantum information, cold atom physics, and precise measurements.^[1–9] In particular, a single-frequency laser source with high power dual-wavelength output is more beneficial to those investigations and measurements. For example, in the generations of squeezed states and entanglements at 1.06 μm, the pump field, the local oscillator, the signal field for the optical parametric amplifier (OPA) or optical parametric oscillator (OPO), and the auxiliary beams used for cavity locking and phase locking can be provided simultaneously by a multi-Watts level single-frequency 1.06 μm and 532 nm dual-wavelength laser.^[10] In precise distance measurements based on heterodyne laser interferometer, the dual-wavelength laser source can be used to compensate the measurement error originated from the instability of the refractive index of the ambient air, and the measurement uncertainty can thus be improved comparing with the single-wavelength laser based interferometer.^[11] Moreover, single-frequency 1.06 μm and 532 nm dual-wavelength lasers can also be used to generate the red-detuning^[12] and blue-detuning^[13] magneto-optical traps for cooling and trapping the atoms, respectively.

Although single frequency lasers with high power 1.06 μm and 532 nm dual-wavelength output have already been demonstrated by using the unidirectional traveling wave

cavity technique and the intracavity second harmonic generation technique,^[14,15] noise reduction techniques and effective power stabilization methods for the dual-wavelength laser sources are still waiting for a detailed study to meet the need of the generation of stable squeezed states and multi-partite entanglements in the audio frequency band, for the reason that the intensity noise and the power fluctuation of the laser source are directly coupled into the response of the photodetectors, and the level of squeezing or entanglement at low frequency is undulated and degraded.

Intensity noise reduction and power stabilization were generally investigated simultaneously in previous works. When a feedback loop based on a combination of an electro-optical amplitude modulator (EOAM) or acousto-optic modulator (AOM) and a polarized beam splitter (PBS) was employed to stabilize the laser power, the laser intensity noise could be suppressed at the same time.^[16–18] Unfortunately, both commercially available and custom made EOAMs or AOMs may lead to a beam quality deterioration of the incident 532 nm laser and the maximum permitted power density of the incident 532 nm laser for an EOAM is generally 0.5 W/mm². Apart from this method, the laser intensity noise can also be reduced by utilizing a mode cleaner (MC) acting as a low-pass filter,^[19,20] but the noise reduction band of the method using MC is restricted by the bandwidth of the MC. Unbalanced Mach-Zehnder interferometer (MZI) is a kind of device that can be used for laser noise suppressing in some discrete frequencies, but not in the audio-frequency region.^[21,22] Con-

*Project supported by the National Key R&D Program of China (Grant No. 2016YFA0301401).

†Corresponding author. E-mail: liyuanji@sxu.edu.cn

© 2019 Chinese Physical Society and IOP Publishing Ltd

<http://iopscience.iop.org/cpb> <http://cpb.iphy.ac.cn>

sequently, some other method should be developed to build a laser source with low intensity noise in the Hz to kHz range and good power stability, which is of benefit to the generation of squeezed state in the audio-frequency region that can be used in the gravitational wave detection.

In this paper, we demonstrate a noise reduction and frequency stabilization system for an intracavity frequency-doubled laser with multi-Watts output. The configuration of the intracavity frequency-doubled laser to be optimized is simply described in Section 2. In Subsection 3.1, the laser frequency stabilization method based on controlling the linear and nonlinear losses of the laser, as well as employing a feedback loop based on a stable frequency reference is introduced. In Subsection 3.2, a balanced MZI and the feedback loop are designed for reducing the intensity noise of the 532 nm laser in the audio-frequency region without degrading the laser beam quality. The influences of the frequency stabilization and the crucial parameters of the MZI, such as the power splitting ratio of the beam splitters and the locking state of the MZI, on the intensity noise of the 532 nm laser are investigated in detail.

2. Experimental setup

The experimental setup of the high power cw single-frequency intracavity frequency-doubled laser and stabilization system is shown in Fig. 1. The pump source is a commercially available laser diode (model: LIMO-A 1294, LIMO) with the center wavelength of 808 nm and a maximal output power of 60 W. Pump light passing through a fiber with core diameter of 400 μm and a collimated lens (f_1) is split

into two beams with orthogonal polarizations by a polarized beam splitter (PBS_1). The reflected pump beam and the transmitted pump beam whose polarization is rotated 90° by a half wave plate (HWP_1) are both focused into the gain medium via two identical focusing lenses (f_2). The gain medium is an a -cut Nd:YVO₄ crystal with a cross-section of 3 mm \times 3 mm \times 20 mm and the Nd concentration of 0.2 at.%. Both end-faces of the Nd:YVO₄ crystal are anti-reflection (AR) coated at 808 nm and 1.06 μm ($R_{808\text{ nm}} < 3\%$ and $R_{1.06\ \mu\text{m}} < 0.2\%$). To suppress the oscillation of the σ -polarization mode and eliminate the etalon effect, a wedge shape of 1.5° is cut on one end-face of the crystal with respect to the c -axis of the crystal. For longitudinal mode selection, a ring resonator composed of 6 mirrors (M_1 – M_6) and an optical diode formed by a HWP_2 and a Faraday rotator based on a terbium gallium garnet (TGG) are employed. The four plane mirrors (M_1 , M_2 , M_3 , M_6) are high reflection (HR) coated at 1.06 μm and high transmission (HT) coated at 808 nm (45° , $R_{1.06\ \mu\text{m}} > 99.8\%$, and $T_{808\text{ nm}} > 95\%$). M_4 and M_5 are concave mirrors with curvature radii of 100 mm, where M_4 is HR coated at 1.06 μm ($R_{1.06\ \mu\text{m}} > 99.8\%$) and fixed onto a piezoelectric-transducer (PZT₁) to control the cavity length, M_5 acting as the output coupler is partially transmission coated at 1.06 μm . A type-I noncritical phase-matched LBO crystal with dimensions of 3 mm \times 3 mm \times 18 mm is chosen for intracavity frequency doubling because of its high damage threshold and large temperature and angular acceptances. The lithium triborate (LBO) crystal with two end-faces AR coated at 1.06 μm and 532 nm ($R_{532\text{ nm}, 1.06\ \mu\text{m}} < 0.25\%$) is inserted

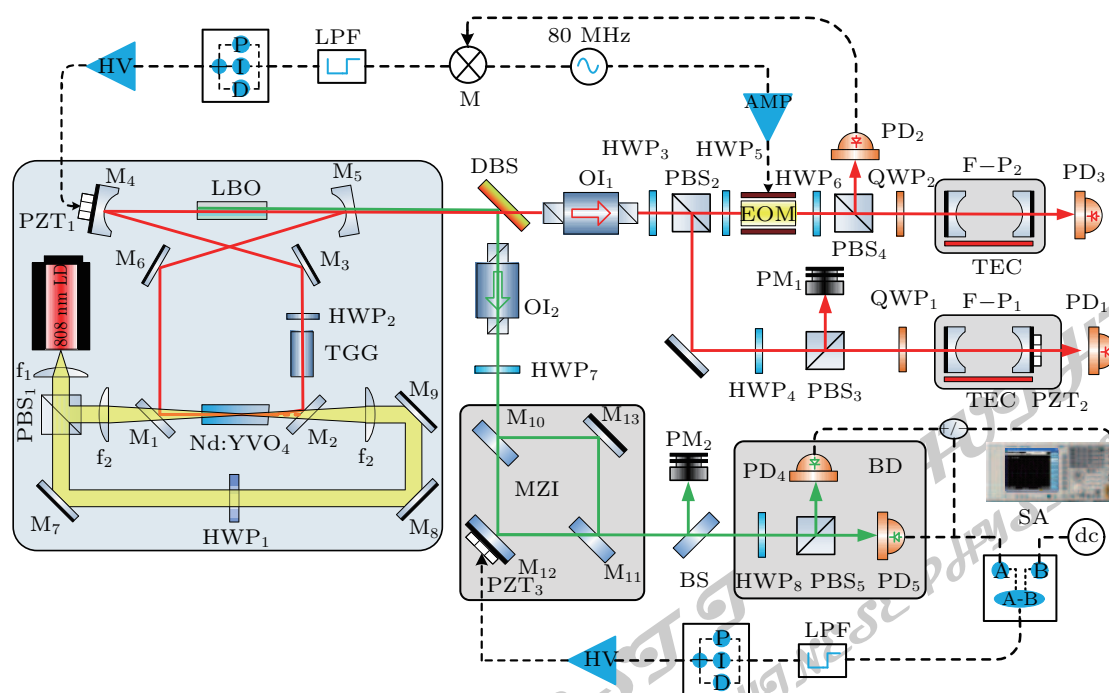


Fig. 1. Experimental setup of high power cw single-frequency dual-wavelength laser and stabilization system. LPF: low pass filter; M: mixer; HV: high voltage amplifier; AMP: power amplifier; dc: direct current source; OI: optical isolator; EOM: electro-optic modulator; PID: proportional-integral-derivative amplifier; A and B: negative power combiner; +/-: positive/negative power combiner; SA: spectrum analyzer.

into the ring cavity at the center of the M_4 – M_5 arm. Both the Nd:YVO₄ and LBO crystals are tightly wrapped with indium for reliable heat transfer and mounted in copper ovens that are temperature controlled using a home-made temperature controller with an accuracy of 0.01 °C. The whole cavity length is 490 mm.

The outputs of fundamental and second harmonic lasers are isolated from the laser resonator using two optical isolators (OIs) and separated using a dichroic mirror (DBS). The 1.06 μm laser is split into three parts using HWP₃, HWP₄, PBS₂, and PBS₃. One portion is sent to a power meter (PM₁, model: LabMax-Top, Coherent). The other two beams are delivered to a scanning Fabry–Pérot (F–P₁) interferometer (free spectral range: 375 MHz; finesse: 350) for monitoring the longitudinal-mode and to a frequency stabilization system for stabilizing the frequency of the laser, respectively. The 532 nm laser is injected into the power stabilization system based on a MZI to reduce its power fluctuation and intensity noise. The long-term power fluctuation and the intensity noise of the stabilized laser are recorded using PM₂ and a balanced detection (BD) system formed by HWP₈, PBS₅, and a pair of low noise, broadband detectors (PD₄ and PD₅), respectively. The common-mode rejection ratio of the BD system is higher than 40 dB. The sum and difference of the detected ac signals are recorded by a spectrum analyzer (SA, model: N9030 A, Agilent). The sum signal gives the intensity noise power of the laser and the difference signal gives the shot noise limit (SNL).

3. Experimental results and discussion

3.1. Mode-hop-free and frequency stabilized laser operation

Based on our previous work on the modeling of the sufficient condition of stable single frequency laser operation with energy transfer upconversion and excited stimulated absorption taken into account,^[23] and considering the power requirement for building the multi-partite entanglements and squeezed states, an output coupler (M_5 in the laser cavity) with a transmission of 1.3% at 1.06 μm and a transmission higher than 99.5% at 532 nm, as well as an LBO temperature of 149.2 °C, which leads to a nonlinear conversion coefficient of 1.346×10^{-10} m²/W that is far beyond the critical value of 0.373×10^{-11} m²/W, were chosen for the generation of the dual-wavelength laser. Figure 2 shows the measured input–output behavior of the laser and the longitudinal mode spectrum. The results indicate that the 532 nm and 1.06 μm outputs as high as 9.5 W and 3.1 W are achieved simultaneously under 50 W pumping, and there is only one longitudinal mode oscillated stably with no mode hop. The beam quality of the dual wavelength lasers was also measured using a laser beam quality analyzer (model: M2-200-BB; CCD: GRAS-20S4M-C, Spricon), the beam quality factors of the 1.06 μm laser were

$M_x^2 = 1.06$ and $M_y^2 = 1.05$. The beam quality factors of the 532 nm laser were $M_x^2 = 1.09$ and $M_y^2 = 1.12$. The beam spot radius of the 532 nm laser 0.3 m apart from the cavity was about 360 μm, the near-field divergence angle of the 532 nm laser was 5.9 mrad.

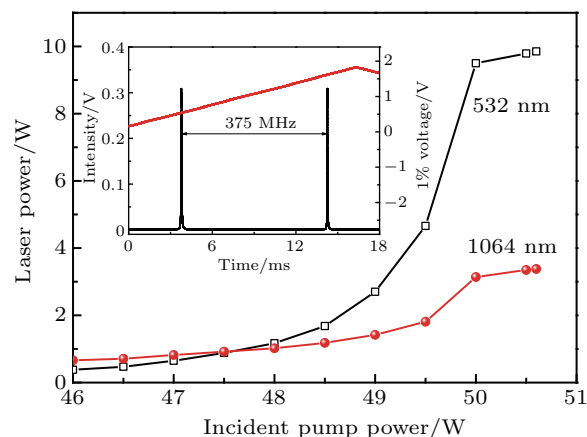


Fig. 2. Output powers of 1.06 μm and 532 nm lasers versus incident pump power. Inset: transmitted intensity of F–P₁ interferometer.

By using a digital oscilloscope (model: DPO7245, Tektronix) and a software based on Labview, the laser frequency deviation from the initial frequency as a function of time was measured and shown in Fig. 3(a). It can be seen that the peak to peak frequency drift of the free running laser during 5 h was about ± 4.8 MHz with no mode hop observed. To further stabilize the laser frequency, a 200 mm-long confocal F–P₂ cavity, which consisted with a tube-shaped invar body and two concave end mirrors with curvature radii of 200 mm, was built as a frequency standard. The finesse of the cavity was measured to be 1000, leading to a linewidth of 375 kHz. Since a temperature fluctuation of the invar body as low as 0.1 °C will cause the resonant frequency to drift within 20 MHz, an active temperature control system was designed and employed to maintain the length of the F–P₂ cavity. The invar tube body was embedded in a copper sheath with an exterior contour of cuboid, whose four side faces were in close contact with eight pieces of thermoelectric cooler (TEC) modules (40 mm×20 mm), and covered by an intermediate polyarylsulfone thermal insulation layer and an outermost aluminum shell acting as heat sink. With the help of a home-made temperature controller, a long term temperature stability of ± 0.003 °C during 5 h was achieved. Based on this robust frequency reference, Pound–Drever–Hall (PDH) frequency locking was demonstrated via a frequency stabilization loop (FSL) as shown in Fig. 1. The fundamental laser beam was firstly phase modulated by an electro-optic modulator (EOM) to generate frequency-modulated sidebands which were 80 MHz apart from the carrier. Then the laser reflected from the F–P₂ cavity was detected by a photo-detector (PD₂),

and the detected signal was multiplied with the local oscillator's signal using a mixer (M) with a phase compensation provided by a delay box. After being filtered by a low-pass filter (LPF), the error signal was obtained and sent to a proportional-integral-derivative (PID) amplifier and a high voltage amplifier (HV) to drive the laser PZT₁. Figure 3(b) shows the frequency drifts of the stabilized laser during 5 h. Once FSL was working, the long term peak to peak frequency drift was less than ± 1.5 MHz.

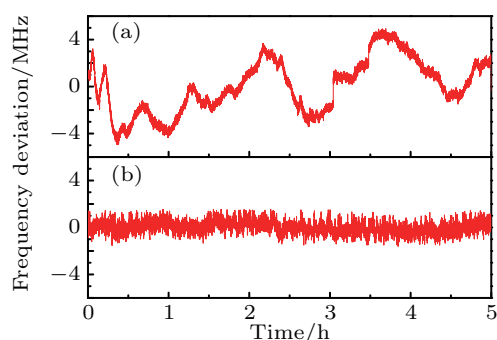


Fig. 3. Frequency drift of (a) free running laser and (b) stabilized laser in 5 h.

3.2. Intensity noise suppression and power stabilization

To stabilize the output power and suppress the intensity noise of the 532 nm laser, a MZI and the corresponding power stabilization loop (PSL) as shown in Fig. 1 were used. The MZI was composed of two HR coated mirrors M₁₂, M₁₃ and two beam splitters (BSs) M₁₀, M₁₁ with a beam splitting ratio of R at 532 nm. The mirror M₁₂ was attached on a PZT₃ for tuning the optical length difference (OPD) between the two arms of the MZI. Then the difference between an adjustable low noise direct current (dc) signal and the low frequency part (dc to 40 kHz) of the detected signal from PD₅ was filtered by a LPF and sent to a PID and a HV to generate the driving signal, which was finally fed back to PZT₃ for locking the OPD. When the voltage of the dc signal was adjusted and the parameters of the proportional-integral-derivative amplifier were tuned accordingly, the transmission of the stabilized laser passing through the MZI (T_{lock}) can be changed. To investigate the influence of the MZI parameters, e.g., T_{lock} and R , on the laser noise properties in the audio frequency region (0.4–30 kHz), the same settings were adopted during the following measurements: Firstly, the laser power incident on PD₄ and PD₅ was kept at 24 μ W. Secondly, the sectional measurements in four Fourier frequency windows including 0.4–0.8 kHz, 0.8–3.2 kHz, 3.2–10 kHz, and 10–30 kHz were carried out for each noise spectrum, and the resolution bandwidths (video bandwidths) of SA in the respective regions were set as 2 Hz (2 Hz), 4 Hz (4 Hz), 16 Hz (4 Hz), and 16 Hz (4 Hz). Thirdly, to reduce the measurement errors, each data point in Figs. 4 and 5 was the averaged value of the data recorded in 400, 400, 800, and 800 measurements for

the four Fourier frequency windows. Fourthly, since the electronic noise was at least 10 dB below the SNL in the frequency region, it had already been subtracted from the measured data.

To investigate the influence of T_{lock} on the laser intensity noise property, the BSs with $R = 50\%$ were used to build the MZI, and the noise spectra were recorded when the OPD of the MZI was locked at different T_{lock} , as shown in Fig. 4. Curves (i) and (ii) are the SNL and intensity noise of the 532 nm laser before the MZI. It can be seen that in the audio frequency region from 0.4 kHz to 30 kHz, the intensity noise of the laser was always higher than the SNL with a difference ranging from 12 dB to 34 dB. Once the 532 nm laser was stabilized using the MZI and PSL, a noise transfer phenomenon was observed. Curves (iii), (iv), and (v) in Fig. 4 are the intensity noises in the laser output from the locked MZI when T_{lock} is 45%, 65%, and 85%, respectively. It can be seen that most of the intensity noise in the laser output from the MZI in the frequency region from 0.7 kHz to 10 kHz was suppressed in all the three cases, while the intensity noise in the frequency region from 10 kHz to 30 kHz was raised up beyond the intensity noise of laser before MZI. Moreover, the amount of noise suppression in the frequency region of 0.7–10 kHz can be adjusted by controlling the locking position of the MZI. As shown in Fig. 4, when T_{lock} was raised up from 45% to 85%, the intensity noise of the laser from 0.7 kHz to 10 kHz was closer to the SNL. In particular, in the analysis frequency region from 0.7 kHz to 3.7 kHz, the intensity noise of laser in the case of $T_{\text{lock}} = 85\%$ was more than 5 dB below that in the case of $T_{\text{lock}} = 45\%$.

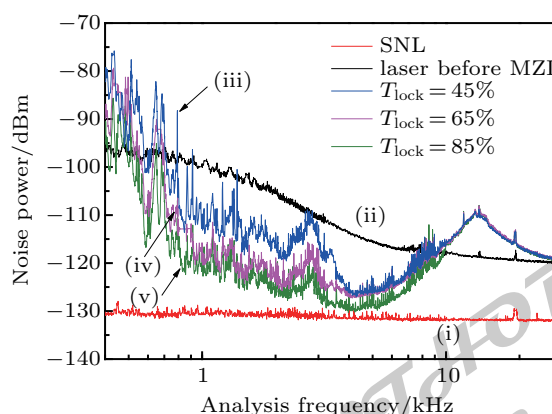


Fig. 4. Intensity noise of laser as a function of analysis frequency when $R = 50\%$.

To test the influence of the beam splitting ratio on the intensity noise of the 532 nm laser, three MZIs with $R = 90\%$, 75%, and 50% were used for 532 nm laser stabilization. Figure 5 shows the measured intensity noises of the laser before the MZI and the stabilized lasers output from the MZIs locked at the same T_{lock} of 85%. Curves (i) and (ii) are the SNL and intensity noise of the laser before the MZI. Curves (iii), (iv),

and (v) are the intensity noises of the lasers output from the locked MZIs when R is 50%, 70%, and 90%, respectively. It can be seen that when the BSs with $R = 90\%$ were used to build the MZI, the intensity noise of the stabilized laser in the frequency region from 0.4 kHz to 3 kHz was further suppressed in comparison with the case of $R = 50\%$, while the intensity noise of the stabilized laser in the frequency region from 3 kHz to 30 kHz became higher.

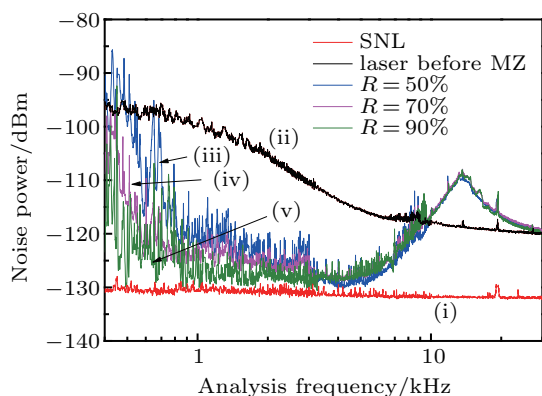


Fig. 5. Intensity noise of laser as a function of analysis frequency with different R of MZI at T_{lock} of 85%.

The influence of laser frequency stabilization on the intensity noise suppression was also measured and shown in Fig. 6. Curves (i) and (ii) are the SNLs of the laser with and without laser frequency stabilization, respectively. Curves (iii) and (iv) are the intensity noises of the laser before the MZI with and without laser frequency stabilization, respectively. Curves (v) and (vi) are the intensity noises of the lasers output from the locked MZIs with and without laser frequency stabilization when R is 90% and T_{lock} is 85%, respectively. It can be seen that the laser frequency stabilization had nearly no influence on the measured SNL and the intensity noise of the laser before MZI. But the intensity noise of the laser after MZI showed significant suppression in the frequency region from 0.4 kHz to 1.3 kHz once the laser was frequency stabilized.

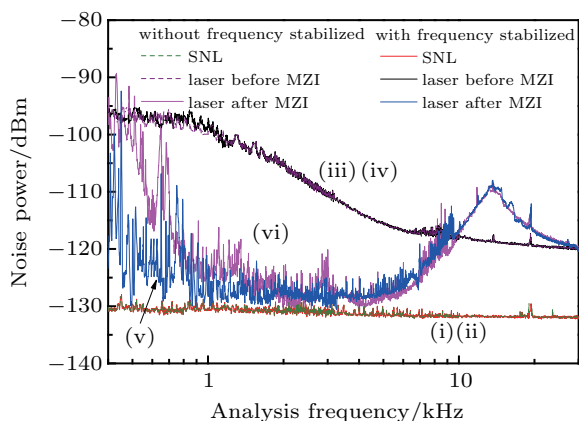


Fig. 6. Intensity noise of laser as a function of analysis frequency in the cases with or without laser frequency stabilization when $R = 90\%$ and $T_{\text{lock}} = 85\%$.

From the above experiment results, the best noise performance was achieved when the laser was frequency stabilized, the MZI with $R = 90\%$ was employed and locked to the state of $T_{\text{lock}} = 85\%$. The performance of laser power stability at the same condition was also measured, as shown in Fig. 7. The measured peak to peak power fluctuation of the 532 nm laser before MZI was less than $\pm 0.7\%$ for a given 5 h. As a comparison, when the 532 nm laser was stabilized via an MZI, the 532 nm output power from the locked MZI was 7.5 W, and the measured peak to peak power fluctuation of laser was less than $\pm 0.2\%$ for a given 5 h.

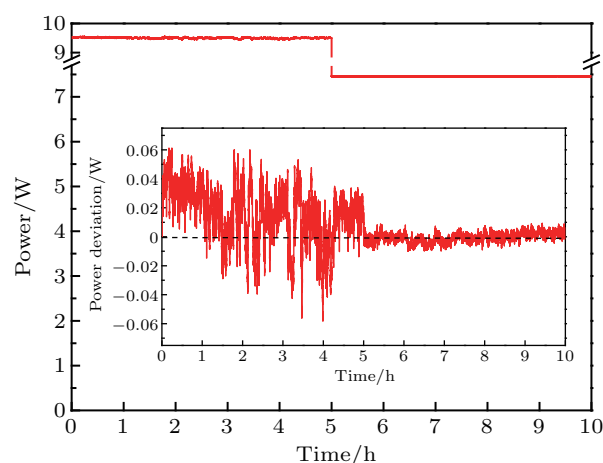


Fig. 7. Power fluctuation of the 532 nm laser before MZI (0–5 h) and output from a locked MZI (5–10 h).

4. Conclusion and perspectives

We built up a high power mode-hop-free cw single-frequency intracavity frequency-doubled Nd:YVO₄/LBO laser, the output power and intensity noise in the audio frequency region of 532 nm laser were stabilized and suppressed via a locked MZI. By utilizing the resonant frequency of a temperature controlled confocal F–P cavity as frequency standard, the frequencies of the dual-wavelength laser were locked via PDH technique, and the measured frequency drift of the 1.06 μm laser was better than ± 1.5 MHz for a given 5 h. Furthermore, a control system based on MZI was designed and used to improve the power stability and the intensity noise property of the 532 nm laser. When the control system was working, the measured power fluctuation was less than $\pm 0.2\%$ during a given 5 h, and the intensity noise was significantly suppressed in the audio frequency region by optimizing the locking level and the beam splitting ratio. Finally, a robust cw single frequency laser operation with 532 nm output of 7.5 W and 1.06 μm output of 3.1 W was achieved. The stable low noise high power cw single-frequency intracavity frequency-doubled laser can satisfy the experimental requirements for the generation of audio frequency band squeezed state and multipartite entanglement. The laser can also be applied in the fields of quantum information and precise measurements.

References

- [1] Kómár P, Kessler E M, Bishof M, Jiang L, Sørensen A S, Ye J and Lukin M D 2014 *Nat. Phys.* **10** 582
- [2] Shuman E S, Barry J F and DeMille D 2010 *Nature* **467** 820
- [3] Liu L W, Gengzang D J, An X J and Wang P Y 2018 *Chin. Phys. B* **27** 034205
- [4] Goda K, Miyakawa O, Mikhailov E E, Saraf S, Adhikari R, McKenzie K, Ward R, Vass S, Weinstein A J and Mavalvala N 2008 *Nat. Phys.* **4** 472
- [5] Fan H Y, Xu X X and Hu L Y 2009 *Chin. Phys. B* **18** 5139
- [6] Shao B, Xiang S H and Song K H 2009 *Chin. Phys. B* **18** 0418
- [7] Wu Q, Xiao Y and Zhang Z M 2015 *Chin. Phys. B* **24** 104208
- [8] Feng J X, Li Y J and Zhang K S 2018 *Chin. Phys. B* **27** 074211
- [9] Zhang Y C, Fan L, Wei C F, Gu X M and Ren S X 2018 *Acta Phys. Sin.* **67** 024206 (in Chinese)
- [10] Vahlbruch H, Mehmet M, Danzmann K and Schnabel R 2016 *Phys. Rev. Lett.* **117** 110801
- [11] Meiners-Hagen K, Meyer T, Mildner J and Pollinger F 2017 *Appl. Phys. Lett.* **111** 191104
- [12] Kuhr S, Alt W and Schrader D 2001 *Science* **293** 278
- [13] Nikolov A N, Eyler E E, Wang X T, Li J, Wang H, Stwalley W C and Gould P L 1999 *Phys. Rev. Lett.* **82** 703
- [14] Jin P X, Lu H D, Su J and Peng K C 2016 *Appl. Opt.* **55** 3478
- [15] Zhang C W, Lu H D, Yin Q W and Su J 2014 *Appl. Opt.* **53** 6371
- [16] Tricot F, Phung D H, Lours M, Guérandel S and Clercq E 2018 *Rev. Sci. Instrum.* **89** 113112
- [17] Junker J, Oppermann P and Willke B 2017 *Opt. Lett.* **42** 755
- [18] Kwee P, Willke B and Danzmann K 2011 *Opt. Lett.* **36** 3563
- [19] Shi Z and Su X L 2010 *Acta Sin. Quantum Opt.* **16** 158 (in Chinese)
- [20] Liu Q, Feng J X, Li H, Jiao Y C and Zhang K S 2012 *Chin. Phys. B* **21** 104204
- [21] Inoue S and Yamamoto Y 1997 *Opt. Lett.* **22** 328
- [22] Zhang X Y, Li Z Y and Li Y M 2015 *Acta Photon. Sin.* **44** 0827001
- [23] Ma Y Y, Li Y J, Feng J X and Zhang K S 2018 *Opt. Express* **26** 1538

JUST FOR AUTHORS
— CHINESE PHYSICS B

Chinese Physics B

Volume 28

Number 9

September 2019

TOPICAL REVIEW — A celebration of the 100th birthday of Kun Huang

098506 Homogeneous and inhomogeneous magnetic oxide semiconductors

Xiao-Li Li and Xiao-Hong Xu

TOPICAL REVIEW — Strong-field atomic and molecular physics

094208 Influence of intraband motion on the interband excitation and high harmonic generation

Rui-Xin Zuo, Xiao-Hong Song, Xi-Wang Liu, Shi-Dong Yang and Wei-Feng Yang

SPECIAL TOPIC — Strong-field atomic and molecular physics

093202 Trajectory analysis of few-cycle strong field ionization in two-color circularly polarized fields

Yan Huang, Chaochao Qin, Yizhu Zhang, Xincheng Wang, Tian-Min Yan and Yuhai Jiang

093301 Coulomb exploded directional double ionization of N₂O molecules in multicycle femtosecond laser pulses

Junyang Ma, Kang Lin, Qinying Ji, Wenbin Zhang, Hanxiao Li, Fenghao Sun, Junjie Qiang, Peifen Lu, Hui Li, Xiaochun Gong and Jian Wu

094207 Quantum interference of multi-orbital effects in high-harmonic spectra from aligned carbon dioxide and nitrous oxide

Hong-Jing Liang, Xin Fan, Shuang Feng, Li-Yu Shan, Qing-Hua Gao, Bo Yan, Ri Ma and Hai-Feng Xu

094212 Atomic even-harmonic generation due to symmetry-breaking effects induced by spatially inhomogeneous field

Yue Guo, Aihua Liu, Jun Wang and Xueshen Liu

TOPICAL REVIEW — 110th Anniversary of Lanzhou University

097504 Techniques of microwave permeability characterization for thin films

Xi-Ling Li, Jian-Bo Wang and Guo-Zhi Chai

SPECIAL TOPIC — 110th Anniversary of Lanzhou University

090503 Quasi-periodic events on structured earthquake models

Bin-Quan Li, Zhi-Xi Wu and Sheng-Jun Wang

097501 Dynamical anisotropic magnetoelectric effects at ferroelectric/ferromagnetic insulator interfaces

Yaojin Li, Vladimir Koval and Chenglong Jia

098802 The effect of Mn-doped ZnSe passivation layer on the performance of CdS/CdSe quantum dot-sensitized solar cells

Yun-Long Deng, Zhi-Yuan Xu, Kai Cai, Fei Ma, Juan Hou and Shang-Long Peng

(Continued on the Bookbinding Inside Back Cover)

REVIEW

098801 An overview of progress in Mg-based hydrogen storage films

Lyu Jinzhe, Andrey M Lider and Viktor N Kudiiarov

RAPID COMMUNICATION

098505 Manipulation of superconducting qubit with direct digital synthesis

Zhi-Yuan Li, Hai-Feng Yu, Xin-Sheng Tan, Shi-Ping Zhao and Yang Yu

GENERAL

090201 Painlevé integrability of the supersymmetric Ito equation

Feng-Jie Cen, Yan-Dan Zhao, Shuang-Yun Fang, Huan Meng and Jun Yu

090301 Attacking a high-dimensional quantum key distribution system with wavelength-dependent beam splitter

Ge-Hai Du, Hong-Wei Li, Yang Wang and Wan-Su Bao

090302 Wigner function for squeezed negative binomial state and evolution of density operator for amplitude decay

Heng-Yun Lv, Ji-Suo Wang, Xiao-Yan Zhang, Meng-Yan Wu, Bao-Long Liang and Xiang-Guo Meng

090303 Dipole–dipole interactions enhance non-Markovianity and protect information against dissipation

Munsif Jan, Xiao-Ye Xu, Qin-Qin Wang, Zhe Chen, Yong-Jian Han, Chuan-Feng Li and Guang-Can Guo

090304 Geometrical quantum discord and negativity of two separable and mixed qubits

Tang-Kun Liu, Fei Liu, Chuan-Jia Shan and Ji-Bing Liu

090501 Chaotic analysis of Atangana–Baleanu derivative fractional order Willis aneurysm system

Fei Gao, Wen-Qin Li, Heng-Qing Tong and Xi-Ling Li

090502 Characteristic signal extracted from a continuous time signal on the aspect of frequency domain

Zhi-Fan Du, Rui-Hao Zhang and Hong Chen

090701 Hybrid-triggered consensus for multi-agent systems with time-delays, uncertain switching topologies, and stochastic cyber-attacks

Xia Chen, Li-Yuan Yin, Yong-Tai Liu and Hao Liu

ATOMIC AND MOLECULAR PHYSICS

093101 Adsorption and desorption phenomena on thermally annealed multi-walled carbon nanotubes by XANES study

Camile Rodolphe Tchenguem Kamto, Bridinette Thiodjio Sendja and Jeannot Mane Mane

093102 The substituent effect on the excited state intramolecular proton transfer of 3-hydroxychromone

Yuzhi Song, Songsong Liu, Jiajun Lu, Hui Zhang, Changzhe Zhang and Jun Du

093201 Coherent control of fragmentation of methyl iodide by shaped femtosecond pulse train

Qiu-Nan Tong, De-Hou Fei, Zhen-Zhong Lian, Hong-Xia Qi, Sheng-Peng Zhou, Si-Zuo Luo, Zhou Chen and Zhan Hu

- 093401 Interaction of H_2^+ molecular beam with thin layer graphene foils**
Min Li, Guo-Feng Qu, Yi-Zhou Wang, Zhou-Sen Zhu, Mian-Gong Shi, Mao-Lei Zhou, Dong Liu, Zi-Xu Xu, Ming-Jiang Song, Jun Zhang, Fan Bai, Xiao-Dong Liao and Ji-Feng Han
- 093402 Relativistic electron scattering from freely movable proton/ μ^+ in the presence of strong laser field**
Ningyue Wang, Liguang Jiao and Aihua Liu
- 093701 Dynamical properties of ultracold Bose atomic gases in one-dimensional optical lattices created by two schemes**
Jiang Zhu, Cheng-Ling Bian and Hong-Chen Wang
- ELECTROMAGNETISM, OPTICS, ACOUSTICS, HEAT TRANSFER, CLASSICAL MECHANICS, AND FLUID DYNAMICS**
- 094201 Experimental demonstration of influence of underwater turbulence on ghost imaging**
Man-Qian Yin, Le Wang and Sheng-Mei Zhao
- 094202 Multiple trapping using a focused hybrid vector beam**
Li Zhang, Xiaodong Qiu, Lingwei Zeng and Lixiang Chen
- 094203 $CsPbBr_3$ nanocrystal for mode-locking Tm-doped fiber laser**
Yan Zhou, Renli Zhang, Xia Li, Peiwen Kuan, Dongyu He, Jingshan Hou, Yufeng Liu, Yongzheng Fang and Meisong Liao
- 094204 Stable continuous-wave single-frequency intracavity frequency-doubled laser with intensity noise suppressed in audio frequency region**
Ying-Hao Gao, Yuan-Ji Li, Jin-Xia Feng and Kuan-Shou Zhang
- 094205 Passively Q-switched diode-pumped Tm, Ho:LuVO₄ laser with a black phosphorus saturable absorber**
Linjun Li, Tianxin Li, Long Zhou, Jianying Fan, Yuqiang Yang, Wenqiang Xie and Shasha Li
- 094206 Forward-headed structure change of acetic acid–water binary system by stimulated Raman scattering**
Zhe Liu, Bo Yang, Hong-Liang Zhao, Zhan-Long Li, Zhi-Wei Men, Xiao-Feng Wang, Ning Wang, Xian-Wen Cao, Sheng-Han Wang and Cheng-Lin Sun
- 094209 Refractive index sensor based on high-order surface plasmon resonance in gold nanofilm coated photonic crystal fiber**
Zhen-Kai Fan, Shao-Bo Fang, Shu-Guang Li and Zhi-Yi Wei
- 094210 Pancharatnam–Berry metasurface for terahertz wave radar cross section reduction**
Shao-He Li and Jiu-Sheng Li
- 094211 Resolving multi-orbital effects on high harmonic generation from aligned N₂ molecules in linearly and elliptically polarized intense laser fields**
Hong-Jing Liang, Xin Fan, Shuang Feng, Li-Yu Shan, Qing-Hua Gao, Bo Yan, Ri Ma, Hai-Feng Xu and Da-Jun Ding

094213 Diode-pumped Kerr-lens mode-locked Ti: sapphire laser with broad wavelength tunability

Han Liu, Geyang Wang, Ke Yang, Renzhu Kang, Wenlong Tian, Dacheng Zhang, Jiangfeng Zhu, Hainian Han and Zhiyi Wei

094214 Comparison of three kinds of polarized Bessel vortex beams propagating through uniaxial anisotropic media

Jia-Wei Liu, Hai-Ying Li, Wei Ding, Lu Bai, Zhen-Sen Wu and Zheng-Jun Li

094215 Properties of metal–insulator–metal waveguide loop reflector

Hu Long, Xuan-Ke Zeng, Yi Cai, Xiao-Wei Lu, Hong-Yi Chen, Shi-Xiang Xu and Jing-Zhen Li

094216 Polarization dependence of gain and amplified spontaneous Brillouin scattering noise analysis for fiber Brillouin amplifier

Kuan-Lin Mu, Jian-Ming Shang, Li-Hua Tang, Zheng-Kang Wang, Song Yu and Yao-Jun Qiao

094217 Quantum optical interferometry via general photon-subtracted two-mode squeezed states

Li-Li Hou, Jian-Zhong Xue, Yong-Xing Sui and Shuai Wang

094301 Using Helmholtz resonator arrays to improve dipole transmission efficiency in waveguide

Liwei Wang, Li Quan, Feng Qian and Xiaozhou Liu

094701 Strong coupling between height of gaps and thickness of thermal boundary layer in partitioned convection system

Ze-Peng Lin and Yun Bao

PHYSICS OF GASES, PLASMAS, AND ELECTRIC DISCHARGES

095201 Fluctuation of arc plasma in arc plasma torch with multiple cathodes

Zelong Zhang, Cheng Wang, Qiang Sun and Weidong Xia

095202 Enhancement of corona discharge induced wind generation with carbon nanotube and titanium dioxide decoration

Jianchun Ye, Jun Li, Xiaohong Chen, Sumei Huang and Wei Ou-Yang

095203 First polar direct-drive exploding-pusher target experiments on the ShenGuang laser facility

Bo Yu, Jiamin Yang, Tianxuan Huang, Peng Wang, Wanli Shang, Xiumei Qiao, Xuewei Deng, Zhanwen Zhang, Zifeng Song, Qi Tang, Xiaoshi Peng, Jiabin Chen, Yulong Li, Wei Jiang, Yudong Pu, Ji Yan, Zhongjing Chen, Yunsong Dong, Wudi Zheng, Feng Wang, Shaoen Jiang, Yongkun Ding and Jian Zheng

CONDENSED MATTER: STRUCTURAL, MECHANICAL, AND THERMAL PROPERTIES

096101 Van der Waals interlayer potential of graphitic structures: From Lennard–Jones to Kolmogorov–Crespy and Lebedeva models

Zbigniew Koziol, Grzegorz Gawlik and Jacek Jagielski

096201 Surperhard monoclinic BC₆N allotropes: First-principles investigations

Nian-Rui Qu, Hong-Chao Wang, Qing Li, Yi-Ding Li, Zhi-Ping Li, Hui-Yang Gou and Fa-Ming Gao

096401 Crystal melting processes of propylene carbonate and 1,3-propanediol investigated by the reed-vibration mechanical spectroscopy for liquids

Li-Na Wang, Xing-Yu Zhao, Heng-Wei Zhou, Li Zhang and Yi-Neng Huang

096402 Structural transitions in NaNH_2 via recrystallization under high pressure

Yanping Huang, Xiaoli Haung, Xin Wang, Wenting Zhang, Di Zhou, Qiang Zhou, Bingbing Liu and Tian Cui

096501 Laser scattering, transmittance and low thermal expansion behaviors in $\text{Y}_{2-x}(\text{ZnLi})_x\text{Mo}_3\text{O}_{12}$ by forming regular grains

Xian-Sheng Liu, Yong-Guang Cheng, Bao-He Yuan, Er-Jun Liang and Wei-Feng Zhang

CONDENSED MATTER: ELECTRONIC STRUCTURE, ELECTRICAL, MAGNETIC, AND OPTICAL PROPERTIES

097401 Josephson effect in the strontium titanate/lanthanum aluminate junction

Xing Yang, Jie Chen, Yabin Yu and Quanhui Liu

097502 The unique magnetic damping enhancement in epitaxial $\text{Co}_2\text{Fe}_{1-x}\text{Mn}_x\text{Al}$ films

Shu-Fa Li, Chu-Yuan Cheng, Kang-Kang Meng and Chun-Lei Chen

097503 Magnetic properties of the double perovskite compound Sr_2YRuO_6

N. EL Mekkaoui, S. Idrissi, S. Mtougui, I. EL Housni, R. Khalladi, S. Ziti, H. Labrim and L. Bahmad

097801 Improvement of TE-polarized emission in type-II $\text{InAlN-AlGaIn}/\text{AlGaIn}$ quantum well

Yi Li, Youhua Zhu, Meiyu Wang, Honghai Deng and Haihong Yin

INTERDISCIPLINARY PHYSICS AND RELATED AREAS OF SCIENCE AND TECHNOLOGY

098101 Characteristics of urea under high pressure and high temperature

Shuai Fang, Hong-An Ma, Long-Suo Guo, Liang-Chao Chen, Yao Wang, Lu-Yao Ding, Zheng-Hao Cai, Jian Wang and Xiao-Peng Jia

098201 The n-type Si-based materials applied on the front surface of IBC-SHJ solar cells

Jianhui Bao, Ke Tao, Yiren Lin, Rui Jia and Aimin Liu

098202 Structural and dielectric properties of giant dielectric $\text{Na}_{1/2}\text{Sm}_{1/2}\text{Cu}_3\text{Ti}_4\text{O}_{12}$ ceramics prepared by reactive sintering methods

H Mahfoz Kotb

098501 Efficient molecular model for squeeze-film damping in rarefied air

Cun-Hao Lu, Pu Li and Yu-Ming Fang

098502 Thermal resistance matrix representation of thermal effects and thermal design of microwave power HBTs with two-dimensional array layout

Rui Chen, Dong-Yue Jin, Wan-Rong Zhang, Li-Fan Wang, Bin Guo, Hu Chen, Ling-Han Yin and Xiao-Xue Jia

098503 Performance improvement of 4H-SiC PIN ultraviolet avalanche photodiodes with different intrinsic layer thicknesses

Xiaolong Cai, Dong Zhou, Liang Cheng, Fangfang Ren, Hong Zhong, Rong Zhang, Youdou Zheng and Hai Lu

- 098504 Intrinsic transverse relaxation mechanisms of polarized alkali atoms enclosed in radio-frequency magnetometer cell**
Yang-Ying Fu and Jie Yuan
- 098701 Terahertz coherent detection via two-color laser pulses of various frequency ratios**
Xin-Yang Gu, Ke-Jia Wang, Zhen-Gang Yang and Jin-Song Liu
- 098901 A new cellular automaton model accounting for stochasticity in traffic flow induced by heterogeneity in driving behavior**
Xiaoyong Ni and Hong Huang

JUST FOR AUTHORS
— CHINESE PHYSICS B